Experimental evaluation of anisotropic dynamic and static elastic modulus in deep Longmaxi shale

Lichun Jia
Drilling & Production Technology Research Institute of CNPC Chuanqing Drilling Engineering Company Limited, Guanghan, People's Republic of China

Hu Deng
Drilling & Production Technology Research Institute of CNPC Chuanqing Drilling Engineering Company Limited, Guanghan, People's Republic of China

ABSTRACT: Understanding the anisotropic elastic properties of deep Longmaxi shale is crucial for analysis of wellbore stability and hydraulic fracturing in this reservoir. Here, the anisotropic dynamic and static elastic properties are measured under dry, soaked by water-based and oil-based drilling fluid conditions. The results show that the anisotropy parameters ε, γ and δ calculated from wave velocities are <<1 for dry or soaked samples, indicating that this shale is a weak anisotropic rock. And the dynamic Young's modulus E_{11} substantially exceeds E_{33} in all cases and both increases with confining pressure. From compression tests, the static Young's modulus $E_{0°}$, $E_{45°}$, $E_{90°}$ increase with confining pressure but decrease dramatically of soaked samples. In conclusion, the dynamic Young's moduli exceed static values regardless of direction, confining pressure, dry or soaked condition. And factors affecting the anisotropy of deep shale include the lower amount of clay content and less clumped clay minerals bands.

Keywords: deep Longmaxi shale, transversely isotropic, ultrasonic wave measurement, uniaxial and triaxial compression tests, dynamic elastic modulus, static elastic modulus.

1 INTRODUCTION

The deep Longmaxi shale, with burial depth of more than 3500m, has been the major target plays in recent years. It is generally recognized that this shale is a typical transversely isotropic (TI) rock with well-developed weak-planes and micro-fractures (Gui et al. 2018 and Dong et al. 2019). For drilling and completion in this reservoir, understanding the anisotropy is important to analyse boreholes stability and design of hydraulic fracturing. There has been a significant amount of studies on measuring the anisotropic properties of rocks, including velocity measurements and uniaxial/triaxial tests (Song et al. 2004, Zadeh et al. 2017 and Condon et al. 2020). In the dynamic tests, five velocities $V_P(0°)$, $V_P(45°)$, $V_P(90°)$, $V_S(0°)$ and $V_{SH}(90°)$, measured from core plugs at three different directions, are needed to calculate the five independent elastic stiffness C_{11}, C_{33}, C_{44}, C_{66} and C_{13} (Mokhtari et al. 2016 and Lozovyi & Bauer 2019). With all the five velocities, dynamic Young's moduli and Poisson's ratio can be obtained (Mavko et al. 2009). Also, the Thomsen parameters ε, γ and δ can be used to characterize the anisotropy of a TI medium (Thomsen 1986). These three parameters have

values smaller than 0.5, but frequently much smaller, which are useful in quantifying anisotropy. While in the static methods, the static elastic moduli directly obtained from the uniaxial/triaxial tests. In general, a set specimens cored with different angles are tested to measure Young's moduli and Poisson's ratio in different direction (Mokhtari et al. 2016, Condon et al. 2020).

Because of different strain magnitudes, strain rates and stress paths used in dynamic and static tests, the dynamic stiffness is found to be larger than the static stiffness (Sone & Zoback 2013 and Mokhtari et al, 2016). Usually, the stress amplitude during static rock compression is typically on the order of 10^{-3} m/m while the stress amplitude of acoustic-wave propagation is typically < 10^{-6} m/m (Lozovyi & Bauer, 2019). This stress amplitude effect is the main reason causing a significant static–dynamic discrepancy. In engineering practice, it often requires the static elastic properties. Thus, to link static and dynamic rock properties, empirical correlations are often used.

For Longmaxi shale, there are numerous studies that examine the anisotropic properties under static conditions and velocity measurement (Heng et al. 2015, Wu et al. 2016 and Dong et al. 2019). But, there are rare investigations on comparison between the dynamic and static elastic modulus in deep Longmaxi shale. To better evaluate the anisotropic dynamic and static elastic modulus in deep shale, the elastic parameters are determined by using ultrasonic and static tests in this study. All shale samples are tested using *0°*, *45°* and *90°* oriented plugs to obtain a full stiffness characterization. And dry, soaked by water-based drilling fluid (WBM) and oil-based drilling fluid (OBM) samples are tested to evaluate the effect of fluid on elastic modulus, respectively. Finally, the correlation of dynamic and static Young's moduli and Poisson's ratios are obtained from these tests, which could be used in analysis of wellbore stability and hydraulic fracturing in filed.

2 SAMPLES AND EXPERIMENTAL METHODS

2.1 Samples characterization

Shale samples are recovered at depth of 4007.90~4008.18m from a deep shale well at Sichuan Basin in China. The average bulk density of this organic-rich black shale is 2.643g/cm^3. The porosity of the samples ranges from 4.3% to 5.5%, and the measured permeability varies from 3.2×10^{-10} to 1.113×10^{-6} mD. The average total organic carbon (TOC) is 3.9%. The XRD analysis shows that this shale is mainly composed of 50.45% quartz minerals, 6.14% plagioclase, 4.80% calcite, 8.25% dolomite, 28.04% clay minerals and minor amount 2.32% Pyrite. In addition, the major component of clay minerals is 59.67% illite, 18.06%chlorite, 1.12%kaolinite and 21.34% mixed layer illite/smectite. And there is no smectite.

2.2 Ultrasonic wave measurement

In velocity measurements, three orientated shale plugs with 25.4 mm diameter by 50 mm length are cut from the full size cores in vertical (θ=0°), horizontal (θ=90°) and diagonal (θ=45°) directions (Figure 1). To avoid any anisotropy induced by a differential stress, a hydrostatic stress state is used to measure velocity (Condon et al. 2020). During measurements, the hydrostatic confining pressure varies from 0 to 80MPa in 20MPa increments at room temperature. Under each target confining pressure, waveforms are recorded after a waiting 3min to stabilize in the pressure vessel.

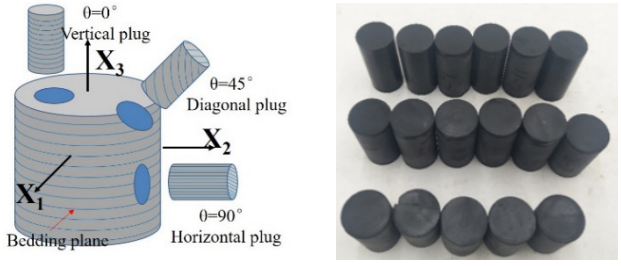

Figure 1. The full size shale core and plugs samples in different orientation.

In addition, to evaluate the effect of drilling fluid soaking on elastic modulus, other two sets of samples soaked 12h by water-based drilling fluid (WBM) and oil-based drilling fluid (OBM), are tested in velocity measurements, respectively. And Table 1 lists the critical parameters of these drilling fluids. It should be noted that these soaked samples are after completely dried to test wave velocities. In summary, there are three groups of samples in velocity measurement, one group is the dry samples while other two are soaked samples. For each group, containing three shale plugs in *0°*, *90°* and *45°* angles, five velocities $V_P(0°)$, $V_P(45°)$, $V_P(90°)$, $V_S(0°)$ and $V_{SH}(90°)$ are measured to calculate the elastic stiffness C_{11}, C_{33}, C_{44}, C_{66} and C_{13}, Thomsen parameters ε, γ and δ and dynamic Young's modulus E_{11}, E_{33} and Poisson's ratios v_{12} and v_{31}.

Table 2. The critical parameters of water-based drilling fluid (WBM) and oil-based drilling fluid (OBM).

Drilling fluid	Density	AV	PV	YP	Gel	HTHP-FL	Vo	pH
WBM (Potassium based)	2.20g/cm^3	69mPa·s	48mPa·s	21Pa	4/12Pa	4.0mL	/	9
OBM (Diesel based)	2.15g/cm^3	56mPa·s	42mPa·s	4Pa	2/7.5Pa	2.2mL	85%	10

2.3 Uniaxial and triaxial compression tests

In the static tests, two sets of *0°*, *45°* and *90°* oriented core plugs are tested in uniaxial and triaxial compression to obtain static Young's modulus $E_{0°}$, $E_{45°}$, $E_{90°}$ and static Poisson's ratios $v_{0°}$, $v_{45°}$, $v_{90°}$, respectively. And the hydrostatic confining pressure of triaxial compression is 80MPa. Meanwhile, the other two sets of samples soaked 12h by water-based drilling fluid and oil-based drilling fluid also are tested in the compression. Similarly, there are three groups of *0°*, *45°* and *90°* oriented shale samples in uniaxial and triaxial tests, respectively. A group is the dry samples while other two groups are soaked samples by different drilling fluid.

3 EXPERIMENTAL RESULTS

3.1 Ultrasonic velocity, elastic stiffness and Thomsen parameters

Figure 2 plots five velocities $V_P(0°)$, $V_P(45°)$, $V_P(90°)$, $V_S(0°)$ and $V_{SH}(90°)$ versus confining pressures for dry and soaked samples. It is very clearly shown that all three P-wave and two S-wave velocities increase with confining pressure. And the increase gradient before 40MPa confining pressure is higher than that after 40MPa. Meanwhile, P-wave velocities parallel to bedding are greater than those in perpendicular and oblique directions. Similarly, S-wave velocity parallel to bedding is higher than that in perpendicular direction. And the order of five velocities is in the follows specific sequence, $V_P(0°)<V_P(45°)<V_P(90°)$ and $V_S(0°)<V_{SH}(90°)$. In addition, all five velocities of soaked samples are lower than those of original dry samples. The results are consistent with the previous results of shallow Longmaxi shales (Gui et al. 2018 and Dong et al. 2019). On the other hand, the decrease gradient of OBM soaked samples is lower than the WBM soaked samples.

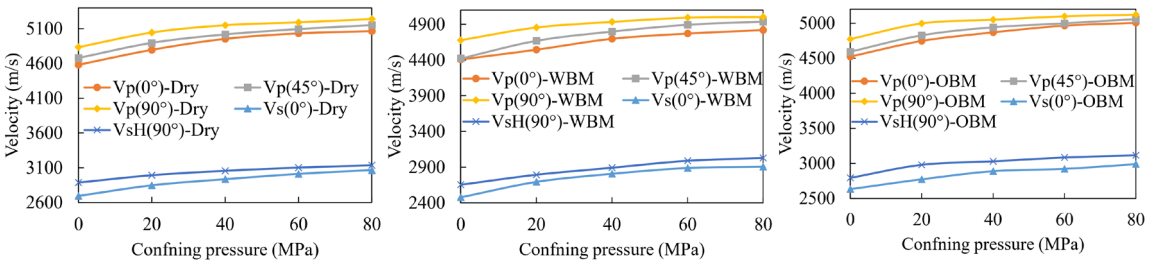

(a) Dry samples (b) Samples soaked in WBM (c) Samples soaked in OBM

Figure 2. Three P-wave and two S-wave velocities of deep Longmaxi shale versus confining stress.

Five independent elastic stiffness C_{11}, C_{33}, C_{44}, C_{66} and C_{13} are calculated directly from the five velocities and are shown in Figure 3. As can be seen, the five elastic constants gradually increase with confining pressure. And the following result of $C_{11}>C_{33}>C_{66}>C_{44}>C_{13}$ is obtained. Moreover, the elastic stiffness of soaked samples are lower than those of dry samples. Similarly, the decrease gradient of OBM soaked samples is lower than the WBM soaked samples.

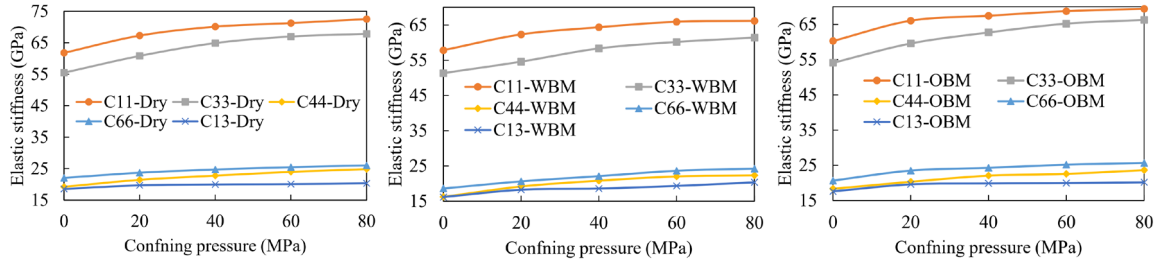

(a) Dry samples (b) Samples soaked in WBM (c) Samples soaked in OBM

Figure 3. Five elastic stiffnesses of deep Longmaxi shale versus confining stress.

The Thomsen parameters ε, γ and δ are calculated from elastic stiffness and shown in Figure 4. The parameters ε and γ decrease with confining pressure, although there are fluctuations in the soaked samples. For the parameter δ, there is no significant change trend with confining pressure. But in a word, the Thomsen parameters ε, γ and δ are <<1 for dry or soaked samples. This indicates that the deep Longmaxi shale is a weak anisotropic rock.

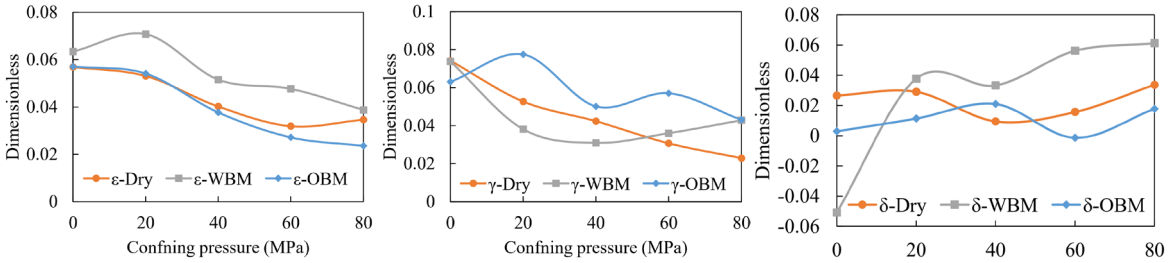

(a) Thomsen parameter ε (b) Thomsen parameter γ (c) Thomsen parameter δ

Figure 4. Thomsen parameters of deep Longmaxi shale versus confining stress.

3.2 *Dynamic and static elastic properties*

The dynamic Young's moduli E_{11}, E_{33} and Poisson's ratios v_{12}, v_{31} are calculated from elastic stiffness (Figure 5). Note that Young's moduli E_{11}, E_{33} and Poisson's ratios v_{12} and v_{31} are parallel and perpendicular to bedding, respectively. As shown in the figure, the Young's moduli increases with confining pressure and E_{11} substantially exceeds E_{33} in all cases. Meanwhile, the drilling fluids would lower Young's moduli in all parallel and perpendicular to bedding. But for the Poisson's ratios, the anisotropy is not obvious and there is no significant change trend with confining pressure.

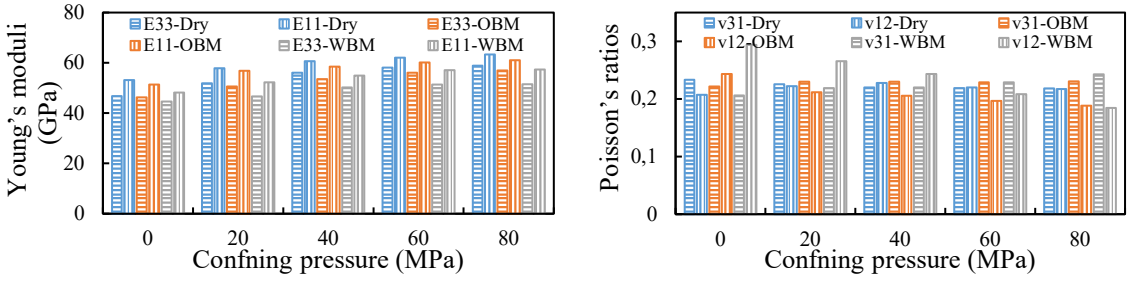

(a) Dynamic Young's moduli (b) Dynamic Poisson's ratios

Figure 5. Dynamic Young's moduli and Poisson's ratios of deep Longmaxi shale versus confining stress.

Figure 6 presents the static Young's modulus $E_{0°}$, $E_{45°}$, $E_{90°}$ and Poisson's ratios $v_{0°}$, $v_{45°}$, $v_{90°}$ from static tests. For static Young's modulus: (1) except for 45° angle sample soaked by WBM, the $E_{0°}$, $E_{45°}$, $E_{90°}$ increase as the angles to bedding increases; (2) Young's modulus in the higher confining pressure substantially exceed those in uniaxial compression; (3) in the soaked condition, the Young's modulus decrease for samples at all angles and the sequence is E(soaked in WBM)< E(soaked in OBM)< E(Dry). However, there is no significant change trend for the Poisson's ratios.

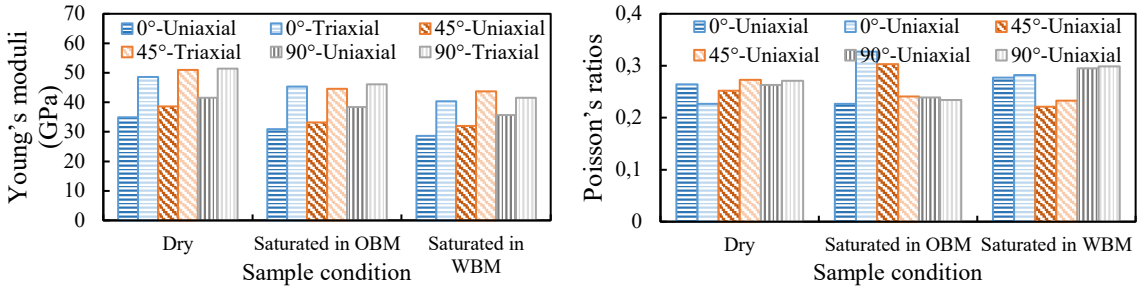

(a) Static Young's moduli (b) Static Poisson's ratios

Figure 6. Static Young's moduli and Poisson's ratios deep Longmaxi shale under dry and soaked condition.

3.3 *The ratio of dynamic and static elastic modulus*

From the velocity measurement and uniaxial/triaxial compression, the dynamic and static elastic modulus of deep Longmaxi shale are collected under dry and soaked condition. Figure 7 illustrates the ratio of dynamic and static Young's moduli and Poisson's ratios for *0°* and *90°* angles samples at 0MPa and 80MPa confining pressure, respectively. In general, dynamic Young's moduli exceed static results regardless of direction, confining pressure, dry or soaked condition. However, Poisson's ratios show the opposite results, that is the dynamic value is lower than the static data.

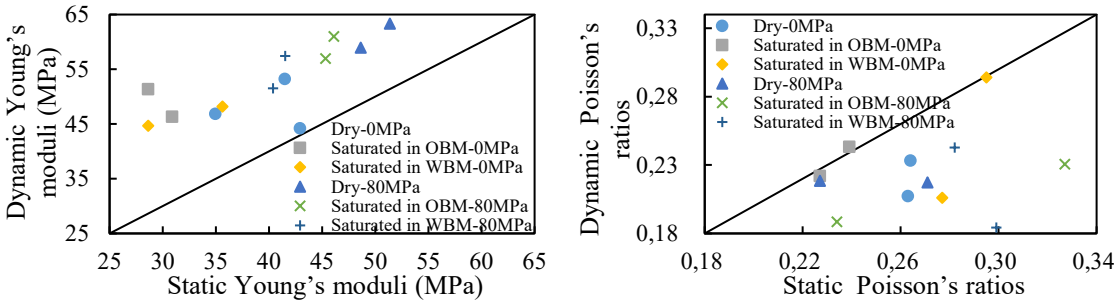

(a) Static Young's moduli (b) Static Poisson's ratios

Figure 7. The correlation of dynamic and static Young's moduli and Poisson's ratios.

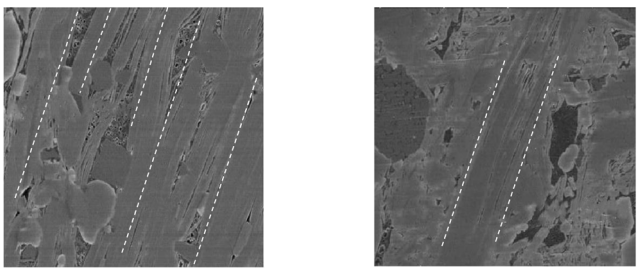

(a) shallow Longmaxi shale (b) deep Longmaxi shale

Figure 8. The SEM image of directionally arranged clay minerals in deep and other Longmaxi shale.

Due to the difference of burial depth, the clay minerals of deep Longmaxi shale in this study is 28.04%, which is lower than 39% clay minerals in the shallow Longmaxi shale with burial depth

3000 to 3500m. And Thomsen parameters ε of deep shale is lower than values obtained from Gui et al. (2018), where the ε of Longmaxi shale in Changning is about 0.055 to 0.115 for dry sample, 0.11 to 0.2 for sample soaked 1h in WBM, 0.10 to 0.15 for sample soaked 3h in WBM. As for the deep shale, the lower amount of clay content results in a reduction of anisotropy. On the other hand, the SEM images of directionally arranged clay minerals in deep and other Longmaxi shale are shown in Figure 8. It shows clearly that there are more clumped clay minerals bands in shallow shale than that in deep shale. This could create higher anisotropy of shallow shale. In addition, the deep Longmaxi shale has a lower porosity, ranging from 4.3% to 5.5%, which is lower than the porosity 7.8% of the Changning shale. This in turn would result in the increase of P- and S-wave velocities and could also affect the anisotropy.

4 CONCLUSIONS

This study evaluates the anisotropic behaviour of deep Longmaxi shale using ultrasonic and static tests under dry, soaked by water-based (WBM) and oil-based drilling fluid (OBM) conditions. The results showing that: (1) As the confining pressure is below 40MPa, all five wave velocities increase at a high gradient. After 40MPa, velocities increase slowly with confining pressure. Meanwhile, all velocities of soaked samples are lower than those of dry samples. (2) The anisotropy parameters ε, γ and δ calculated from elastic constants are $<<1$ for dry or soaked samples, indicating that this deep Longmaxi shale is a weak anisotropic rock. (3) The dynamic and static Young's modulus all increase with confining pressure. The Young's modulus parallel to bedding substantially exceeds results of perpendicular to bedding. And the soaked condition will decrease the Young's modulus dramatically. But the anisotropy of Poisson's ratios is not obvious. (4) The factors affecting the anisotropy of deep shale include the lower amount of clay content and less clumped clay minerals bands.

REFERENCES

Condon, K.J., Sone, H. & Wang H.F. 2020. Low static shear modulus along foliation and its influence on the elastic and strength anisotropy of Poorman Schist Rocks, Homestake Mine, South Dakota. *Rock Mechanics and Rock Engineering* 53, pp.5257-5281, from https://doi.org/10.1007/s00603-020-02182-4.

Dong, G.J., Chen, P., Yuan, H.Y. & Lu, Y.D. 2019. The experimental investigation of Longmaxi shale dynamic parameters under water-based mud soaking. *Geofluids 3*, pp.1-12.

Gui, J.C., Ma, T.S., Chen, P., Yuan, H.Y. & Guo, Z.X. 2018. Anisotropic damage to hard brittle shale with stress and hydration coupling. *Energies* 11(4), 926, DOI:10.3390/en11040926.

Heng, S., Guo, Y.T., Yang, C.H., Daemen, J.J.K. & Li, Z. 2015. Experimental and theoretical study of the anisotropic properties of shale. *International Journal of Rock Mechanics & Mining Sciences* 74, pp.58-68.

Lozovyi, S. & Bauer, A. 2020. From static to dynamic stiffness of shales: frequency and stress dependence. *Rock Mechanics and Rock Engineering* 52, pp.5085-5098.

Mokhtari, M., Honarpour, M.M., Tutuncu, A.N. & Boitnott, G.N. 2016. Characterization of elastic anisotropy in Eagle Ford shale: impact of heterogeneity and measurement scale. *SPE Reservoir Evaluation & Engineering* 19 (03), pp.429-439.

Mavko, G., Mukerji, T. & Dvorkin, J. 2009. *Rock physics handbook: Tools for seismic analysis of porous media*. In-house publisher: Cambridge University press.

Sone, H. & Zoback, M.D. 2013. Mechanical properties of shale-gas reservoir rocks - Part 1: Static and dynamic elastic properties and anisotropy. *Geophysics* 78(5), pp.381-392.

Song, I., Suh. M., Woo, Y.K. & Hao, T.Y. 2004. Determination of the elastic modulus set of foliated rocks from ultrasonic velocity measurements. *Engineering Geology* 72, pp.293-308.

Thomsen, L. 1986. Weak elastic anisotropy. *Geophysics* 51, pp.1954-1966. DOI: 10.1190/1.1442051.

Wu, Y.S., Li, X., He, J.M. & Zheng, B. 2016. Mechanical properties of Longmaxi black organic-rich shale samples from south China under uniaxial and triaxial compression states. *Energies* 9, 1088. DOI:10.3390/en9121088.

Zadeh, M.K., Mondol, N.H., Jahren, J. 2017. Velocity anisotropy of Upper Jurassic organic-rich shales, Norwegian Continental Shelf. *Geophysics* 82(2), pp.61-75.